Inorg. Chem. **2007**, *46*, 9569–9574

Synthesis, Crystal Structure, and Magnetic Properties of Hexanuclear $[\{ML_2\}_4\{Nb(CN)_8\}_2]$ and Nonanuclear $[\{ML_2\}_6\{Nb(CN)_8\}_3]$ Heterometallic Clusters (L = bpy, phen)

Thengarai S. Venkatakrishnan,[†] Raghunathan Rajamani,[‡] S. Ramasesha,*[,‡] and Jean-Pascal Sutter*[,†]

Laboratoire de Chimie de Coordination du CNRS, Université Paul Sabatier, 205 route de Narbonne, 31077 Toulouse, France, and Solid State and Structural Chemistry Unit, Indian Institute of Science, Bangalore 560012, India

Received December 13, 2006

A hexanuclear cyano-bridged $\{Mn^{II}_4Nb^{IV}_2\}$ cluster (**1**) bearing 2,2′-bipyridine (bpy) as the blocking ligand at manganese is obtained from the reaction of *cis*-$[MnCl_2(bpy)_2]$ and $K_4[Nb(CN)_8]$. When the blocking ligand is 1,10-phenanthroline (phen), a nonanuclear cluster $\{Mn^{II}_6Nb^{IV}_3\}$ (**2**) is obtained. The structure of $[\{Mn(bpy)_2\}_4\{Nb(CN)_8\}_2]$ has been solved by single-crystal X-ray crystallography, whereas the phen derivative has been confirmed by means of the structure analysis of the corresponding W^{IV} analogue $[\{Mn(phen)_2\}_6\{W(CN)_8\}_3(H_2O)_2]$. Magnetic measurements revealed $S = 9$ and $^{27}/_2$ spin ground states for these aggregates as a result of antiferromagnetic Nb–Mn interaction with $J_{Nb-Mn} = -18.1$ cm^{-1} (**1**) and -13.6 cm^{-1} (**2**).

Introduction

The past decade has witnessed immense research interest in the rational design and synthesis of low-dimensional supramolecular magnetic architectures possessing large-spin ground states. Such assemblies are believed to have relevance in information storage at the molecular level. The importance of such supramolecular architectures is more prominent when the spin in the ground state is large and anisotropic ($D < 0$ and small E), thereby exhibiting slow relaxation of the magnetization below a blocking temperature and behaving as single-molecule magnets (SMMs).[1] The approach of combining molecular modules to obtain chemical architectures of different dimensions, topology, and composition provides an accessible route to modifying their magnetic properties. Such a logical bottom-up approach has been used extensively to prepare bimetallic magnets,[2,3] and to date, a large number of magnetic supramolecular architectures of various dimensionalities are known. The majority of the reports on such materials have largely utilized cyanide as the bridging ligand for exchange of magnetic information.[4] Examples of clusters with large-spin ground states include the $\{M^{II}_9M'^{V}_6\}$ clusters that are derived from molybdenum(V) and tungsten(V) octacyanometalate building blocks;[5−8] the corresponding $\{Co_9M'_6\}$ cluster with a $S = {}^{21}/_2$ spin ground state exhibits SMM behavior.[9,10] The strategy to obtain low-dimensional architecture is to utilize building units in which certain sites are blocked by ligands, thereby directing the process to form such aggregates.[11−21]

* To whom correspondence should be addressed. E-mail: ramasesh@sscu.iisc.ernet.in (S.R.), sutter@lcc-toulouse.fr (J.-P.S.).
† Université Paul Sabatier.
‡ Indian Institute of Science.

(1) Gatteschi, D.; Sessoli, R. *Angew. Chem., Int. Ed.* **2003**, *42*, 269−297.
(2) Mathonière, C.; Sutter, J.-P.; Yakhmi, J. V. In *Magnetism: Molecules to Materials*; Miller, J. S., Drillon, M., Eds.; Wiley-VCH: Weinheim, Germany, 2002; Vol. 4, pp 1−40.
(3) Verdaguer, M.; Girolami, G. S. In *Magnetism: Molecules to Materials*; Miller, J. S., Drillon, M., Eds.; Wiley-VCH: Weinheim, Germany, 2005; Vol. 5, pp 283−346.
(4) Verdaguer, M.; Bleuzen, A.; Train, C.; Garde, R.; Fabrizi de Biani, F.; Desplanches, C. *Philos. Trans. R. Soc. London A* **1999**, *357*, 2959−2976.
(5) Larionova, J.; Gross, M.; Pilkington, M.; Andres, H.; Stoeckli-Evans, H.; Güdel, H. U.; Decurtins, S. *Angew. Chem., Int. Ed.* **2000**, *39*, 1605−1609.
(6) Zhong, Z. J.; Seino, H.; Mizobe, Y.; Hidai, M.; Fujishima, A.; Ohkoshi, S.-I.; Hashimoto, K. *J. Am. Chem. Soc.* **2000**, *122*, 2952−2953.
(7) Bonadio, F.; Gross, M.; Stoeckli-Evans, H.; Decurtins, S. *Inorg. Chem.* **2002**, *41*, 5891−5896.
(8) Lim, J. H.; Yoon, J. H.; Kim, H. C.; Hong, C. S. *Angew. Chem., Int. Ed.* **2006**, *45*, 7424−7426.
(9) Song, Y.; Zhang, P.; Ren, X.-M.; Shen, X.-F.; Li, Y.-Z.; You, X.-Z. *J. Am. Chem. Soc.* **2005**, *127*, 3708−3709.
(10) Freedman, D. E.; Bennett, M. V.; Long, J. R. *Dalton Trans.* **2006**, 2829−2834.
(11) Fehlhammer, W. P.; Fritz, M. *Chem. Rev.* **1993**, *93*, 1243−1280.
(12) Dunbar, K. R.; Heintz, R. A. In *Progress in Inorganic Chemistry*; Karlin, K. D., Ed.; John Wiley & Sons, Inc.: New York, 1997; Vol. 45, pp 283−391.
(13) Shores, M. P.; Sokol, J. J.; Long, J. R. *J. Am. Chem. Soc.* **2002**, *124*, 2279−2292.

10.1021/ic062383t CCC: $37.00
Published on Web 10/02/2007

A major issue for supramolecular magnetic materials remains the temperature at which the magnetic properties are expressed. Indeed, the desired magnetic features are generally obtained at temperatures far below the temperatures at which the smart material devices are required to operate, mainly because of weak exchange interactions. In direct relation with this problem, the use of metal ions of the second and third transition series to achieve stronger exchange interactions between the spin carriers is currently investigated. For Cr^{III}, Mo^{V}, and W^{V} cyano-bridged compounds, an increase of the exchange strength with Ni^{II} has been evidenced following the trend 3d < 4d < 5d, with the W^{V} derivative exhibiting an exchange coupling twice as strong as its Cr^{III} 3d homologue.[13,22] In 3D frameworks, such ions have permitted obtainment of magnets with T_c's above 100 K.[23] As part of this investigation, we consider the Nb^{IV} 4d ion. Very few examples of exchange-coupled compounds involving this spin carrier have been reported so far.[15,24] Herein we describe a series of manganese−niobium clusters $[Mn^{II}_{2x}Nb^{IV}_{x}]$ formed by the self-assembly of $\{Nb(CN)_8\}^{4-}$ and $\{Mn^{II}(L)_2\}$ (L = chelating nitrogen ligand) building units. Their magnetic behaviors are analyzed and discussed.

Results and Discussion

Synthesis and Structural Features. The reaction of *cis*-$[MnCl_2(bpy)_2]$, where bpy stands for 2,2′-bipyridine, with $K_4[Nb(CN)_8]$ in acetonitrile−water solutions results in the formation of the hexanuclear cluster $[\{Mn(bpy)_2\}_4\{Nb(CN)_8\}_2]\cdot 15H_2O$ (**1**). On the other hand, the reaction with *cis*-$[MnCl_2(phen)_2]$, where phen stands for 1,10-phenanthroline, in acetonitrile−water solutions results in the formation of the nonanuclear cluster $[\{Mn(phen)_2\}_6\{Nb(CN)_8\}_3(H_2O)_2]\cdot 24H_2O$ (**2**). Slow interdiffusion of the reagent solutions yielded for **1** single crystals suitable for X-ray diffraction studies, but crystals of cluster **2** had poor diffraction and the structure could not be solved. However, considering that $\{M(CN)_8\}^{4-}$ with either M = Nb^{IV}, Mo^{IV}, or W^{IV} leads to isostructural analogues under identical assembling conditions,[15,24−28] we prepared the cluster $[\{Mn(phen)_2\}_6\{W(CN)_8\}_3(H_2O)_2]\cdot 21H_2O$ (**3**) from *cis*-$[MnCl_2(phen)_2]$ and $K_4[W(CN)_8]$. The IR spectra for compounds **2** and **3** are identical[29] (see the Supporting Information), confirming the analogy between them. The formula analogy is also confirmed by the chemical analyses and by the magnetic data for **2**. Powder X-ray diffraction recorded for compound **2** revealed that the solid is totally amorphous but the structure of **3** was established by single-crystal X-ray diffraction. It can be mentioned that the $\{Nb(CN)_8\}^{4-}$ building unit is prone to decomposition more than $\{W(CN)_8\}^{4-}$. When the diffusion process leading to $\{Mn_4Nb_2\}$ and $\{Mn_6Nb_3\}$ was maintained for a longer time, unidentified side products were observed. To avoid these impurities, it is important to stop the crystal growth process after a few days (see the Experimental Section); such a limitation was not observed for the W derivative.

Compound **1** crystallizes in the *P*2/*c* space group, and there are two independent molecules in the asymmetric unit (A and B). A plot of the molecular structure for **1** is shown in Figure 1, together with a view of the central core. The molecular structure consists of a hexanuclear cluster made up of two $\{Nb(CN)_8\}$ units and four $\{Mn(bpy)_2\}$ moieties. Each $\{Nb(CN)_8\}$ unit is linked to four Mn^{II} ions through four of its cyano ligands, and each Mn center is connected to two Nb units and to two chelating bpy ligands. The central core is best described as an octahedron for which the four Mn ions are located at the corners of the equatorial plane and the Nb ions at the vertices above and below this plane (Figure 1). The overall molecular organization is very similar to the compound formed with $\{Mo(CN)_8\}^{4-}$ and $\{Mn(bpy)_2\}^{2+}$ units, but the latter was found to crystallize in a different space group.[30] The central core is also very reminiscent of the organization found in the 3D frameworks developed during assembly of a $\{M(CN)_8\}^{4-}$ building unit with M^{2+} metal ions.[31] Compound **1** nicely underlines the expected role of the blocking ligands, which is to hinder the growth of an extended structure without affecting the assembling scheme of the complementary building units.

The intramolecular Mn···Mn distances between adjacent nonbonded Mn sites vary between 5.656(5) and 8.497(4) Å for molecule A and between 5.591(4) and 8.392(5) Å for molecule B. In molecule A, the two Nb atoms are located 3.378 and 3.380 Å above and below the plane. In molecule B, these values are 3.450 and 3.447 Å. Apart from the two *cis* bidendate ligands, each Mn is bonded to two N centers of the cyanide ligand (one from each Nb center). The Mn−N(C) distances lie between 2.11 and 2.20 Å. The Mn−N−C

(14) Marvaud, V.; Decroix, C.; Scuiller, A.; Tuyèras, F.; Guyard-Duhayon, C.; Vaissermann, J.; Marrot, J.; Gonnet, F.; Verdaguer, M. *Chem.−Eur. J.* **2003**, *9*, 1692−1705.
(15) Pradhan, R.; Desplanches, C.; Guionneau, P.; Sutter, J.-P. *Inorg. Chem.* **2003**, *42*, 6607−6609.
(16) Wang, S.; Zuo, J.-L.; Zhou, H.-C.; Choi, H.-J.; Ke, Y.; Long, J. R.; You, X.-Z. *Angew. Chem., Int. Ed.* **2004**, *43*, 5940−5943.
(17) Schelter, E. J.; Prosvirin, A. V.; Dunbar, K. R. *J. Am. Chem. Soc.* **2004**, *126*, 15004−15005.
(18) Li, D.; Parkin, S.; Wang, G.; Yee, G. T.; Clérac, R.; Wernsdorfer, W.; Holmes, S. M. *J. Am. Chem. Soc.* **2006**, *128*, 4214−4215.
(19) Li, D.; Parkin, S.; Clérac, R.; Holmes, S. M. *Inorg. Chem.* **2006**, *45*, 7569−7571.
(20) Jiang, L.; Feng, X.-L.; Lu, T.-B.; Gao, S. *Inorg. Chem.* **2006**, *45*, 5018−5026.
(21) Boyer, J. L.; Kuhlman, M. L.; Rauchfuss, T. B. *Acc. Chem. Res.* **2007**, *40*, 233−242.
(22) Visinescu, D.; Desplanches, C.; Imaz, I.; Bahers, V.; Pradhan, R.; Villamena, F.; Guionneau, P.; Sutter, J. P. *J. Am. Chem. Soc.* **2006**, *128*, 10202−10212.
(23) Tanase, S.; Tuna, F.; Guionneau, P.; Maris, T.; Rombaut, G.; Mathonière, C.; Andruh, M.; Kahn, O.; Sutter, J.-P. *Inorg. Chem.* **2003**, *42*, 1625−1631.
(24) Pilkington, M.; Decurtins, S. *Chimia* **2000**, *54*, 593−601.
(25) The shift in the CN stretching frequency by 20 cm^{-1} is normally observed between Nb^{4+} and Mo^{4+}/W^{4+}; see, for instance, refs 15 and 26.
(26) Sieklucka, B.; Podgajny, R.; Przychodzen, P.; Korzeniak, T. *Coord. Chem. Rev.* **2005**, *249*, 2203−2221.
(27) Rombaut, G.; Golhen, S.; Ouahab, L.; Mathonière, C.; Kahn, O. *J. Chem. Soc., Dalton Trans.* **2000**, 3609−3614.
(28) Willemin, S.; Larionova, J.; Clérac, R.; Donnadieu, B.; Henner, B.; LeGoff, X. F.; Guérin, C. *Eur. J. Inorg. Chem.* **2003**, 1866−1872.
(29) Dong, W.; Sun, Y. Q.; Zhu, L.-N.; Liao, D.-Z.; Jiang, Z.-H.; Yan, S.-P.; Cheng, P. *New J. Chem.* **2003**, *27*, 1760−1764.
(30) Sieklucka, B.; Szklarzewicz, J.; Kemp, T. J.; Errington, W. *Inorg. Chem.* **2000**, *39*, 5156−5158.
(31) Tuna, F.; Golhen, S.; Ouahab, L.; Sutter, J.-P. *C. R. Chim.* **2003**, *6*, 377−383.

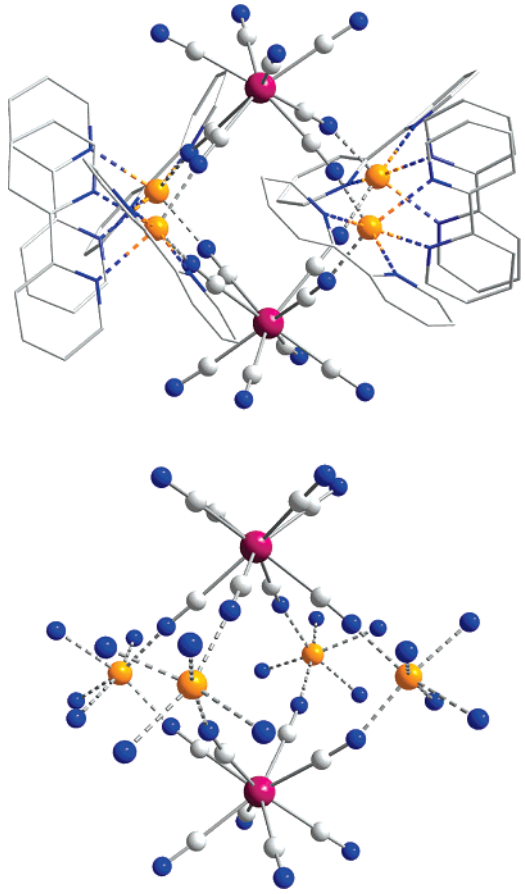

Figure 1. Molecular structure for **1**: (top) one of the two molecules forming the asymmetric unit (Nb in purple and Mn in orange); (bottom) detail of the central cyano-bridged hexanuclear core.

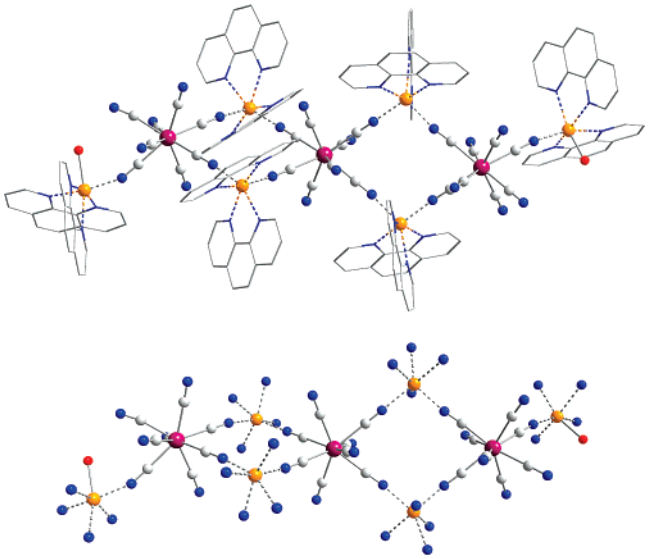

Figure 2. Molecular structure for **3**: (top) asymmetric unit (W in purple and Mn in orange); (bottom) detail of the molecular topology.

angles span from 149 to 175°, whereas the Nb−C−N angles are close to linearity and lie in the range 172.0−179.4°.

Clusters **2** and **3** are isomorphous. The molecular structure of cluster **3** is shown in Figure 2. Interestingly, changing the blocking ligand from bpy to phen has resulted in a different assembling process. The structure can be described as one in which two Mn_2W_2 squares are connected together at the W corner; the central W (W2) is part of both squares. The two squares formed at W2 are oriented at 69.0°. Both of the squares are further connected to one pendant Mn(phen)$_2$(OH$_2$) unit, which stops the assembling process from extending further into a polymeric chain network. The intramolecular nonbonded Mn···Mn and Mn···W distances are in the ranges 6.898−10.535 and 5.323−5.549 Å, respectively. The two W···W distances are 8.551 and 8.439 Å. The W−C−N angles lie in the range 169.1−179.9°, and the Mn−N−C angles are between 157.9 and 176.3°. The Mn−N(C) distances lie between 2.147 and 2.221 Å.

At first glance, it is rather surprising that the $\{Mn(bpy)_2\}^{2+}$ and $\{Mn(phen)_2\}^{2+}$ modules do not lead to the same supramolecular organization during assembly with $\{M(CN)_8\}^{4-}$. The structural features, however, reveal that for the hexanuclear aggregate **1** the bpy units adopt a slightly twisted conformation; i.e., the angle between the two pyridine rings deviates from zero. For phen, such a deformation is not possible and obviously an organization as for compound **1** cannot accommodate this rigid ligand. A different assembling scheme is favored, leading to compounds **2** and **3**.

The polyhedral shape around the Nb centers does not correspond to ideal symmetry [i.e., square antiprism (SAP), dodecahedron (DD), etc.]; therefore, a continuous shape measures (CShM) analysis[32−35] was carried out with SHAPE[36] to ascertain the geometry of the $\{M(CN)_8\}$ moieties. Indeed, the actual shape of the $\{M(CN)_8\}$ polyhedron determines the strength of the exchange interaction mediated by each CN bridge.[22] Analysis of the coordination polyhedra of the cyanometalate core in clusters **1** and **3** shows that the geometry around the metal center is a distorted SAP. In cluster **1**, the coordination spheres for niobium centers Nb1, Nb2, and Nb4 are closer to SAP geometry than to DD geometry, while that of Nb3 has a shape midway between both of these geometries and lies on the path of interconversion between these two limiting geometries. In cluster **3**, all of the three octacyanotungstate units adopt a slightly distorted SAP geometry. The results of the SHAPE analysis have been tabulated in Table S1 in the Supporting Information.

Magnetic Properties of Compounds 1 and 2. The magnetic behaviors for **1** and **2** were investigated on polycrystalline samples in the temperature domain 2−300 K. The temperature dependence of the molar magnetic susceptibility, χ_M, for each compound is given as $\chi_M T$ plots in Figure 3. For **1**, the value for $\chi_M T$ at 300 K is 17.23 cm^3 mol^{-1} K, slightly lower than the expected spin-only value of 18.25 cm^3 mol^{-1} K for four Mn^{II} ions ($S = {}^5/_2$; $g = 2$) and two Nb^{IV} ions ($S = {}^1/_2$; $g = 2$). The $\chi_M T$ value decreases gradually until 204 K, reaching 16.94 cm^3 mol^{-1} K. As the

(32) Alvarez, S.; Alemany, P.; Casanova, D.; Cirera, J.; Llunell, M.; Avnir, D. *Coord. Chem. Rev.* **2005**, *249*, 1693−1708.
(33) Casanova, D.; Llunell, M.; Alemany, P.; Alvarez, S. *Chem.—Eur. J.* **2005**, *11*, 1479−1494.
(34) Casanova, D.; Cirera, J.; Llunell, M.; Alemany, P.; Avnir, D.; Alvarez, S. *J. Am. Chem. Soc.* **2004**, *126*, 1755−1763.
(35) Cirera, J.; Ruiz, E.; Alvarez, S. *Chem.—Eur. J.* **2006**, *12*, 3162−3167.
(36) Llunell, M.; Casanova, D.; Cirera, J.; Bofill, J. M.; Alemany, P.; Alvarez, S.; Pinsky, M.; Avnir, D. *SHAPE*, 1.1b ed.; Barcelona, 2005.

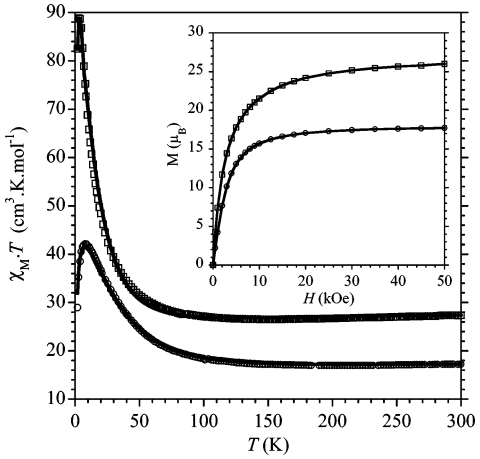

Figure 3. Experimental (○ for **1**; □ for **2**) and calculated (—) $\chi_M T$ vs T behavior for **1** and **2**. Inset: field dependence of the magnetization at 2 K (lines are only eye guides).

temperature is further lowered, the $\chi_M T$ value increases, reaching a maximum value of 42.13 cm^3 mol^{-1} K at 8 K. The $\chi_M T$ product then decreases with a further lowering of the temperature and attains a value of 28.97 cm^3 mol^{-1} K at 2 K. The plot of $\chi_M T$ vs T for cluster **2** displays a behavior similar to that for cluster **1**, with the values at 300, 154, and 3 K being respectively 27.32, 26.52, and 88.80 cm^3 mol^{-1} K. The field dependence of magnetization at 2 K shows that the magnetization reaches a value of 17.72 and 26.01 μ_B at 50 kOe respectively for the clusters **1** and **2**. These values are in line with the anticipated $S = 9$ spin ground state for **1** ($M_S = 18\ \mu_B$) and $S = {}^{27}/_2$ for **2** ($M_S = 27\ \mu$B) as a result of antiferromagnetic Nb−Mn interactions.[15,24] This is also supported by the $\chi_M T$ vs T behavior that exhibits a maximum value (42.13 cm^3 mol^{-1} K) for compound **1** close to the value of 45 cm^3 mol^{-1} K anticipated for a $S = 9$ spin state, while for compound **2**, the $\chi_M T$ value reaches 88.80 cm^3 mol^{-1} K versus 97.88 cm^3 mol^{-1} K for a $S = {}^{27}/_2$ spin state.

We have shown recently that an accurate analysis of the magnetic behavior of compounds involving paramagnetic $\{M(CN)_8\}^{3-}$ units necessitates taking into consideration the local geometry of the unit. Depending on its shape, the CN ligands may not be equivalent as far as the transfer of the magnetic information is concerned and, consequently, one or more exchange pathways should be considered during analysis of the magnetic behavior.[22] The CShM analysis performed for compounds **1** and **3** (see above) has established that the polyhedron defining the octacyanometalates is best described by a distorted SAP. In this geometry, symmetry considerations reveal that all of the cyanides of the $\{M(CN)_8\}$ unit are equivalent; hence, the exchange interaction mediated by them should be the same. Therefore, we have analyzed the behavior of compounds **1** and **2** by considering a single mean $Nb^{IV}-Mn^{II}$ exchange parameter, J_{NbMn}. To account for the decrease of $\chi_M T$ at low temperatures, both intermolecular interactions (zJ') and the zero-field-splitting effect (D) have been considered.

The spin Hamiltonian employed to model the spins in the Mn_6Nb_3 system **2** is given by $H = -J(\mathbf{S}_{Nb1}\cdot\mathbf{S}_{Mn1} + \mathbf{S}_{Nb1}\cdot\mathbf{S}_{Mn2} + \mathbf{S}_{Nb1}\cdot\mathbf{S}_{Mn3} + \mathbf{S}_{Nb2}\cdot\mathbf{S}_{Mn2} + \mathbf{S}_{Nb2}\cdot\mathbf{S}_{Mn3} + \mathbf{S}_{Nb2}\cdot\mathbf{S}_{Mn4} + \mathbf{S}_{Nb2}\cdot\mathbf{S}_{Mn5} + \mathbf{S}_{Nb3}\cdot\mathbf{S}_{Mn4} + \mathbf{S}_{Nb3}\cdot\mathbf{S}_{Mn5} + \mathbf{S}_{Nb3}\cdot\mathbf{S}_{Mn6}) - zJ'\langle\mathbf{S}_z^{tot}\rangle\sum_i\mathbf{S}_i^z + g\mu_B\mathbf{H}\sum_i\mathbf{S}_i^z + \mathbf{D}\mathbf{S}_z^2$, where J is the intramolecular exchange constant between the Mn and Nb ions, J' is the intermolecular interaction parameter, z is the number of nearest neighbors of a molecule in the crystal, and **S**'s are the spin operators acting on the Nb or Mn site (Figure 4). Our notation corresponds to J (or J') negative, antiferromagnetic, and J (or J') positive, ferromagnetic. The first term in the Hamiltonian refers to the exchange interaction between the Mn and Nb sites, while the second term corresponds to the intermolecular interaction in the mean-field approximation. The last two terms are the Zeeman and anisotropy terms, respectively. We have neglected the E term in the anisotropy interaction because it is usually much smaller than D and is off-diagonal, leading to energy correlations in higher order. In the $\{Mn_6Nb_3\}$ system, the spin on each Nb ion is ${}^1/_2$ and that on each Mn is ${}^5/_2$. The exchange interaction is between nearest-neighbor Nb and Mn ions. The anisotropic interaction terms as well as the magnetic field and intermolecular interaction terms are very weak compared to the intramolecular exchange interactions. Therefore, we treat all of the terms except the exchange interaction as a perturbation over the exchange Hamiltonian. The spin system has a very large number of possible orientations; for example, in the case of $\{Mn_6Nb_3\}$, this is 6^62^3 and obtaining all of the eigenvalues is computationally prohibitive. This can be judged by the fact that the total $M_S = {}^1/_2$ Hilbert space dimensionality is 33 786 and solving for all of the eigenvalues in this sector is computationally very intense. However, the dimensionality of the total $S = {}^1/_2$ space is much smaller (1642). Indeed, the largest subspace encountered is for the case of total spin $S = {}^9/_2$ and has a dimensionality of 4650. Thus, if we can set up the Hamiltonian matrix in the total spin basis, it is possible to obtain all of the eigenstates and consequently compute accurate thermodynamic properties. However, using a method such as the valence-bond (VB) method, in which the total spin states are explicitly constructed by exploiting Rumer−Pauling rules, for this purpose is fraught with difficulties. The exchange operator operating on a VB state gives rise to states that cannot be easily decomposed into basis states, as discussed elsewhere.[37] In order to avoid these difficulties, we have followed the method of finding the transformation between VB diagrams that obeys Rumer−Pauling rules and the states in the constant M_S basis. With this transformation, we block diagonalize the Hamiltonian in the $M_S = {}^1/_2$ sector into blocks in different spin spaces.

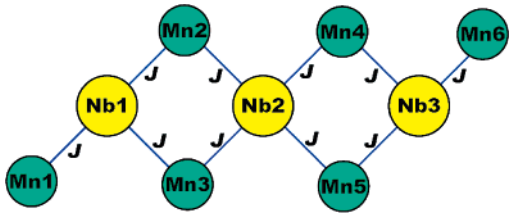

Figure 4. Exchange scheme for the $\{Mn_6Nb_3\}$ system. J's represent the intramolecular interaction constants between the Mn and Nb ions.

(37) Pati, S. K.; Ramasesha, S.; Sen, D. In *Magnetism: Molecules to Materials*; Miller, J. S., Drillon, M., Eds.; Wiley-VCH: New York, 2002; Vol. 4.

We diagonalize each block fully to obtain all of the eigenstates in the spin sector to which the block belongs. The magnetic susceptibility is given by[38]

$$\chi = \frac{N_A g^2 \mu_B{}^2 F(J,T)}{k_B T - zJ' F(J,T)}$$

where μ_B is the Bohr magneton, k_B is the Boltzmann constant, N_A is Avogadro's number, and g is the gyromagnetic ratio, taken to be 2.0. The function $F(J,T)$ is given by

$$F(J,T) = \frac{\sum_S \sum_{M_S} M_S{}^2 \exp[\{-E_0(S,M_S) - DM_S{}^2\}/k_B T]}{\sum_S \sum_{M_S} \exp[\{-E_0(S,M_S) - DM_S{}^2\}/k_B T]}$$

where E_0 is the energy eigenvalue of the unperturbed Hamiltonian.

The Hamiltonian for the Mn_4Nb_2 system **1** is similarly given by $H = -J(\mathbf{S}_{Nb1}\cdot\mathbf{S}_{Mn1} + \mathbf{S}_{Nb1}\cdot\mathbf{S}_{Mn2} + \mathbf{S}_{Nb1}\cdot\mathbf{S}_{Mn3} + \mathbf{S}_{Nb1}\cdot\mathbf{S}_{Mn4} + \mathbf{S}_{Nb2}\cdot\mathbf{S}_{Mn1} + \mathbf{S}_{Nb2}\cdot\mathbf{S}_{Mn2} + \mathbf{S}_{Nb2}\cdot\mathbf{S}_{Mn3} + \mathbf{S}_{Nb2}\cdot\mathbf{S}_{Mn4}) - zJ'\langle\mathbf{S}_z^{tot}\rangle\sum_i \mathbf{S}_i^z + g\mu_B\mathbf{H}\sum_i \mathbf{S}_i^z + \mathbf{D}\mathbf{S}_z{}^2$. In this system (**1**), all of the Mn ions are in a planar arrangement, with the Nb1 ion above the plane and the Nb2 ion below the plane. We assume exchange interactions only between the Mn and Nb ions. The susceptibility is again computed as before. The best fit to the experimental data (Figure 3) yielded, for **1**, $J_{NbMn} = -18.2$ cm^{-1}, $zJ' = -0.005$ cm^{-1}, and $D = 0.008$ cm^{-1}, and for **2**, the best fit was obtained for $J_{NbMn} = -13.6$ cm^{-1}, $zJ' = -0.01$ cm^{-1}, and $D = 0.020$ cm^{-1} with $g = 2$ (fixed).

The magnetic behaviors of {Mn_4Nb_2}, **1**, and {Mn_6Nb_3}, **2**, are qualitatively and quantitatively in agreement with the anticipated behavior. The antiferromagnetic {$Nb^{IV}CN \rightarrow Mn^{II}$} interaction relies on the overlap between singly occupied 3d orbitals of the Mn^{II} ions and a π orbital of the N atom of the bridging cyanide ligands. For paramagnetic {M(CN)$_8$} in SAP geometry, the CN ligands have been shown to carry significant positive spin density transferred from the central metal ion.[22] The strengths of the exchange interactions deduced from these clusters are the first quantitative data available for Nb in CN-bridged assemblies, and they are in the range of those found for related {Mo^V-Mn^{II}} derivatives.[39] Moreover, the values found for **1** and **2** agree well with the exchange coupling anticipated for a $4d^1$ {M(CN)$_8$} unit in the SAP shape. An investigation of the incidence of the geometry of the {M(CN)$_8$} unit on the spin distribution has shown that the spin population on the cyanide N atoms for SAP geometry is higher than that for the CN located on the A sites of a DD but smaller than the population found on the B-site CN of the DD. The exchange interaction strengths are anticipated to follow the same trend, i.e., $J_{DD-A} < J_{SAP} < J_{DD-B}$.[22] For cyanide-bridged {Mo^V-Mn^{II}} assemblies with DD-shaped {Mo(CN)$_8$} units, Ruiz and coworkers[39] have reported exchange interactions of $J_{DD-A} = -15$ cm^{-1} and $J_{DD-B} = -20$ cm^{-1}. The exchange interactions found for compounds **1**, $J_{NbMn} = -18.2$ cm^{-1}, and **2**, $J_{NbMn} = -13.6$ cm^{-1}, thus agree well with the anticipated trend.

Concluding Remarks

The two hexa- and nonanuclear cyano-bridged {Mn−Nb} compounds **1** and **2** are further providing evidence for the enhanced exchange coupling that can be obtained when using second- or third-row transition metals as spin carriers. An idea of the gain is given by comparing the exchange parameter found for compounds **1** and **2** with that of compounds based on {$Fe^{III}CN$} linkages, where the 3d ion has a low spin with $S = 1/2$ ground state and has antiferromagnetic interaction with Mn^{II}. Several data found in the literature indicate that the {$Fe-CN \rightarrow Mn^{II}$} interaction spans from −0.9 to −8 cm^{-1}, at best twice smaller than the exchange parameters obtained with Nb.[40−42]

The different assembling scheme obtained with the ligands bpy and phen was not anticipated. This opens interesting perspectives for the preparation of compounds with different topologies without affecting the crystal-field effect of the {M′(N∼N)} moieties.

Finally, among the known {M(CN)$_8$}$^{n-}$ compounds, the paramagnetic Nb^{IV} derivative is very seldom considered; however, as demonstrated here, it is certainly a valuable building unit to form supramolecular magnetic architectures such as high-spin aggregates.

Experimental Section

The compounds $K_4[Nb(CN)_8]$,[43] $K_4[W(CN)_8]$,[44] *cis*-[$MnCl_2$-(bpy)$_2$], and *cis*-[$MnCl_2$(phen)$_2$][45] were prepared by reported procedures. The solvents used in the reactions were degassed or distilled under a N_2 atmosphere. IR spectra were recorded as KBr pellets in the range 4000−400 cm^{-1} by using a Perkin-Elmer spectrum GX 2000 FTIR spectrometer. Elemental analyses were performed using a Perkin-Elmer 2400 series II instrument. Magnetic measurements down to 2 K were carried out with a Quantum Design MPMS-5S SQUID susceptometer. All magnetic investigations were performed on polycrystalline samples. The molar susceptibility was corrected for the sample holder and for the diamagnetic contribution of all of the atoms by using Pascal's tables.[38,46]

Synthesis of [{(bpy)$_2$Mn}$_4${Nb(CN)$_8$}$_2$]·15H$_2$O (1). A solution of $K_4[Nb(CN)_8]$ (0.025 g, 0.05 mmol) in water (5 mL) was layered with a solution of *cis*-[$MnCl_2$(bp)$_2$] (0.052 g, 0.1 mmol) in 1:1 MeCN−H_2O (5 mL each). Prism-shaped yellow crystals suitable for single-crystal X-ray diffraction study were obtained after 5 days. The crystals were isolated and washed with water and ether. Yield: 11 mg (9%). *Continuing the crystallization for a longer*

(38) Kahn, O. *Molecular Magnetism*; VCH: Weinheim, Germany, 1993.
(39) Ruiz, E.; Rajaraman, G.; Alvarez, S.; Gillon, B.; Stride, J.; Clérac, R.; Larionova, J.; Decurtins, S. *Angew. Chem., Int. Ed.* **2005**, *44*, 2711−2715.
(40) Lescouezec, R.; Lloret, F.; Julve, M.; Vaissermann, J.; Verdaguer, M. *Inorg. Chem.* **2002**, *41*, 818−826.
(41) Lescouëzec, R.; Vaissermann, J.; Toma, L. M.; Carrasco, R.; Lloret, F.; Julve, M. *Inorg. Chem.* **2004**, *43*, 2234−2236.
(42) Ni, Z.-H.; Kou, H.-Z.; Zhang, L.-F.; Ni, W.-W.; Jiang, Y.-B.; Cui, A.-L.; Ribas, J.; Sato, O. *Inorg. Chem.* **2005**, *44*, 9631−9633.
(43) Kiernan, P. M.; Griffith, W. P. *J. Chem. Soc., Dalton Trans.* **1975**, 2489−2494.
(44) Leipoldt, J. G.; Bok, L. D. C.; Cilliers, P. J. *Z. Anorg. Allg. Chem.* **1974**, *407*, 350−352.
(45) McCann, S.; McCann, M.; Casey, R. M. T.; Kackman, M.; Devereux, M.; McKee, V. *Inorg. Chim. Acta* **1998**, *279*, 24−29.
(46) Baker, J. G. A.; Rushbrooke, G. S.; Gilbert, H. E. *Phys. Rev. A* **1964**, *135*, 1272.

time resulted in the formation of byproducts. Hence, the yield of the isolated compound is low. Anal. Calcd for $C_{96}H_{94}N_{32}Mn_4Nb_2O_{15}$: C, 49.24; H, 4.05; N, 19.14. Found: C, 49.29; H, 3.53; N, 19.00. IR (KBr pellet, $\nu_{C\equiv N}$): 2142(m), 2117(m) cm^{-1}.

Synthesis of [{Mn(phen)$_2$}$_6${Nb(CN)$_8$}$_3$(H$_2$O)$_2$]·24H$_2$O (2). A solution of $K_4[Nb(CN)_8]$ (0.016 g, 0.03 mmol) in water (3 mL) was layered with a solution of *cis*-$[MnCl_2(phen)_2]$ (0.032 g, 0.06 mmol) in 1:1 MeCN−H_2O (3 mL each). The product formed after 4 days was isolated and washed with water and ether. Yield: 14 mg (33%). *Continuing the crystallization for a longer time resulted in the formation of byproducts. Hence, the yield of the isolated compound is low*. Anal. Calcd for $C_{168}H_{148}N_{48}Mn_6Nb_3O_{26}$: C, 52.23; H, 3.86; N, 17.40. Found: C, 52.61; H, 2.71; N, 16.87.[47] IR (KBr pellet, $\nu_{C\equiv N}$): 2142(m), 2120(m) cm^{-1}.

Synthesis of [{Mn(phen)$_2$}$_6${W(CN)$_8$}$_3$(H$_2$O)$_2$]·21H$_2$O (3). A solution of $K_4[W(CN)_8]$ (0.029 g, 0.05 mmol) in water (10 mL) was layered with a solution of *cis*-$[MnCl_2(phen)_2]$ (0.049 g, 0.1 mmol) in 1:1 MeCN−H_2O (5 mL each). Yellow crystals formed after 1 week. The crystals were isolated and washed with water and ether. Yield: 0.031 g (45%). Anal. Calcd for $C_{168}H_{142}N_{48}O_{23}Mn_6W_3$: C, 49.42; H, 3.50; N, 16.46. Found: C, 49.16; H, 3.03; N, 16.19. IR (KBr pellet, $\nu_{C\equiv N}$): 2128, 2107 cm^{-1}.

X-ray Crystallography. A crystal suitable for diffraction was coated with paratone and mounted onto the goniometer, and intensity data were obtained from an XCALIBUR Oxford CCD diffractometer using Mo Kα radiation (0.71073 Å) at 180 K. The unit cell parameters were obtained by means of a least-squares refinement performed on a set of 9479 (**1**) or 6989 (**3**) well-measured reflections. The structures have been solved by direct methods using *SIR92*[48] and refined by means of least-squares procedures on *F* using the PC version of the program *CRYSTALS*.[49] The atomic scattering factors were taken from *International Tables for X-Ray Crystallography*.[50] Absorption correction was performed using the multiscan procedure. For compound **1**, there are two independent molecules in the asymmetric unit. Because of the large number of atoms in the asymmetric unit, anisotropic refinement was performed only on the heavy atoms (Mn and Nb). Several bipyridyl were treated as rigid groups in order to minimize the number of parameters. They were refined using an overall refinable isotropic thermal parameter for each group. H atoms were introduced at calculated positions in the last refinement and refined by using a riding model. For compound **3**, atoms of the "W3Mn6" molecule were refined anisotropically. Solvent molecules were refined isotropically. phen ligands were treated as rigid groups in order to minimize the number of parameters. Eight restraints were applied on distances. H atoms were introduced at calculated positions in the last refinement and refined by using a riding model. The list of selected bond distances and angles are given in the Supporting Information (Tables S2−S5).

Crystallographic details for **1**: $C_{96}H_{87.25}N_{32}O_{11.62}Mn_4Nb_2$, M_r = 2280.73, crystal size 0.07 × 0.15 × 0.27, monoclinic, space group *P*2/*c*, a = 23.923(5) Å, b = 19.690(5) Å, c = 47.387(5) Å, β = 97.776(5)°, V = 22116(8) Å^3, Z = 8, ρ_{calcd} = 1.37 g cm^{-3}, $F(000)$ = 9112, μ(Mo Kα) = 0.71 mm^{-1}. A total of 59 125 reflections were measured in the range 4.00° ≤ 2θ ≤ 58.16°, of which 11 242 were unique (R_{int} = 0.15). Final R indices: R1 = 0.094 [$I < 2\sigma(I)$], wR2 = 0.095 (all data) for 1097 parameters; max/min residual electron density 1.48/−1.11 e Å^{-3}. Crystallographic details for **3**: $C_{168}H_{140.5}N_{48}O_{22.25}Mn_6W_3$, M_r = 4069.00, crystal size 0.08 × 0.10 × 0.30, monoclinic, space group *C*2/*c*, a = 33.759(7) Å, b = 41.862(8) Å, c = 28.543(6) Å, β = 125.59(3)°, V = 32803(17) Å^3, Z = 8, ρ_{calcd} = 1.65 g cm^{-3}, $F(000)$ = 15 920, μ(Mo Kα) = 2.62 mm^{-1}. A total of 43 665 reflections were measured in the range 4.00° ≤ 2θ ≤ 58.18°, of which 17 838 were unique (R_{int} = 0.09). Final R indices: R1 = 0.045 [$I < 2\sigma(I)$], wR2 = 0.051 (all data) for 1780 parameters; max/min residual electron density 2.25/−1.52 e Å^{-3}.

Acknowledgment. This work was supported by the Centre Franco−Indien pour la Promotion de la Recherche Avancée/Indo-French Centre for the Promotion of Advanced Research (CEFIPRA/IFCPAR Project 3108-3) and by the European Union sixth framework program NMP3-CT-2005-515767 entitled "MAGMANet: Molecular Approach to Nanomagnets and multifunctional materials". The authors thank Dr. Carine Duhayon for her assistance in X-ray crystallography. We thank Prof. S. Alvarez, Universitat de Barcelona, for providing us the SHAPE program.

Supporting Information Available: X-ray crystallographic files for clusters **1** and **3** (CIF format) and ORTEP plots, results of SHAPE analysis, selected bond distances and angles, and IR spectra for compounds **1**−**3** (PDF file). This material is available free of charge via the Internet at http://pubs.acs.org.

IC062383T

(47) The slight discrepancy found for the chemical analyses might be ascribed to the presence of traces of the byproduct even for short reaction times. Delaying the isolation led to a rapid deviation from the calculated analysis with time, with the C, H, and N composition becoming less.

(48) Altomare, A.; Cascarano, G.; Giacovazzo, C.; Guagliardi, A. *J. Appl. Crystallogr.* **1993**, *26*, 343−350.

(49) Betteridge, P. W.; Carruthers, J. R.; Cooper, R. I.; Prout, K.; Watkin, D. J. *J. Appl. Crystallogr.* **2003**, *36*, 1487.

(50) *International Tables for X-Ray Crystallography*; Kynoch Press: Birmingham, England, 1974; Vol. IV.